

Supporting information

Design of transition-metal-doped TiO_2 as a multipurpose support for fuel cell applications: using a computational high-throughput material screening approach

Meng-Che Tsai,[†] John Rick,[†] Wei-Nien Su,[‡] and Bing-Joe Hwang^{*,†,§}

[†]Nano Electrochemistry Laboratory, Department of Chemical Engineering, National Taiwan University of Science and Technology, Taipei 106, Taiwan

[‡]Graduate Institute of Applied Science and Technology, National Taiwan University of Science and Technology, Taipei 106, Taiwan

[§]National Synchrotron Radiation Research Center, Hsinchu 30076, Taiwan

*Corresponding author: Bing-Joe Hwang (bjh@mail.ntust.edu.tw)

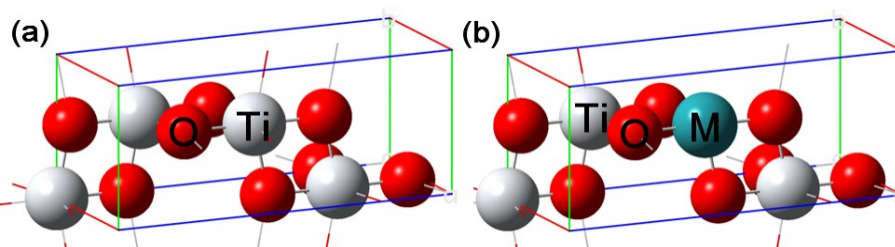


Figure S1 Bulk models of (a) anatase- TiO_2 and (b) anatase- TiMO_2 with 25 atomic percent of dopant M. The atomic ratio in the unit-cell is 3(Ti):1(M):8(O). White, red and Teal balls represent Ti, O and transition metal dopant (M), respectively. These bulk models are used to calculate electronic structure by HSE method.

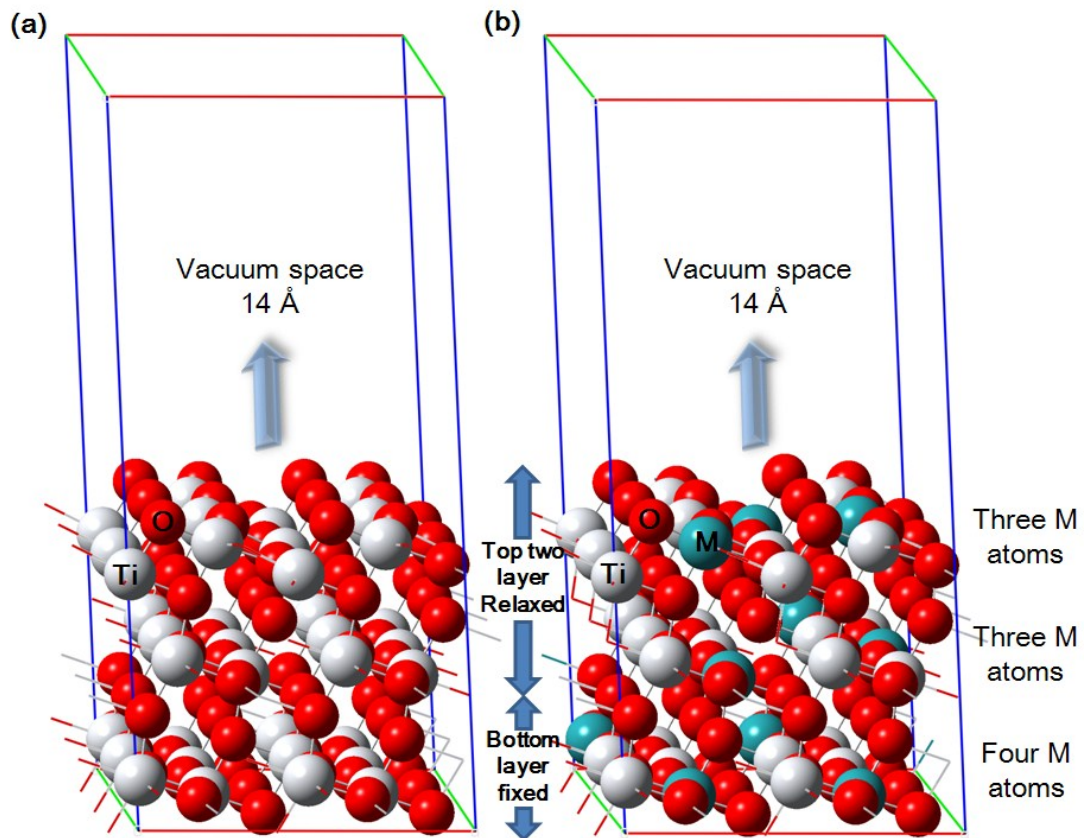


Figure S2 Slab models of (a) anatase-TiO₂ (101), and (b) anatase-TiMO₂ (101) with around 30 atomic percent of dopant M. White, red and Teal balls represent Ti, O and transition metal dopant (M), respectively. Numbers of M on each layer is specified for the different TiMO₂ models.

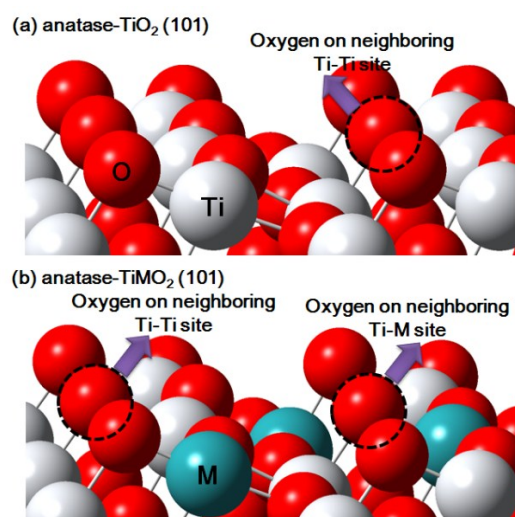


Figure S3 Oxygen vacancy formations, created on (a) neighboring Ti-Ti site of anatase-TiO₂ (101), and (b) neighboring Ti-Ti and Ti-M sites of anatase-TiMO₂ (101). White, red and teal balls represent Ti, O and transition metal dopant (M), respectively.

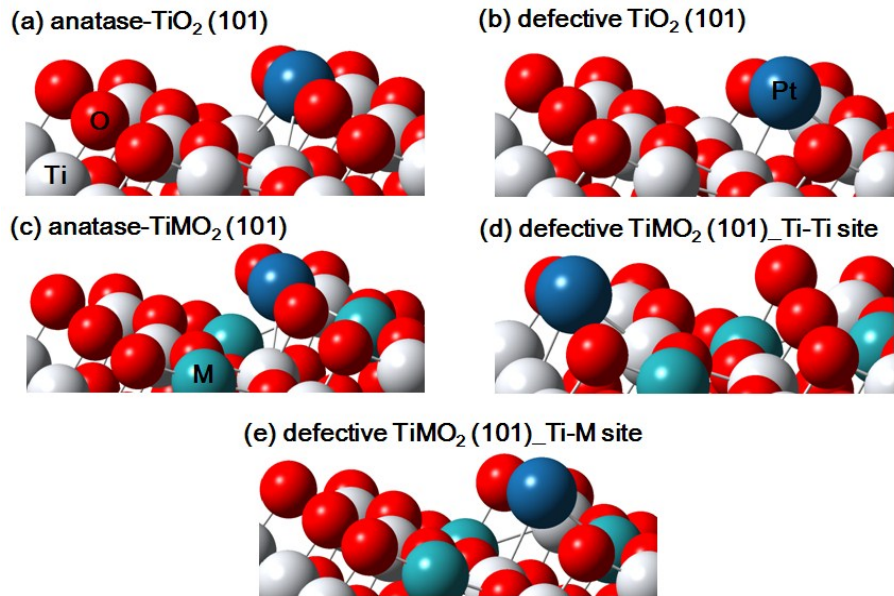


Figure S4 The adsorption configurations for a single Pt adatom on: (a) defect-free site of anatase- TiO_2 , (b) neighboring Ti-Ti site (vacancy) of defective TiO_2 , (c) defect-free site of anatase- TiMO_2 , (d) neighboring Ti-Ti site of defective TiMO_2 and (e) neighboring Ti-M site of defective TiMO_2 . White, red, teal and blue balls represent Ti, O, transition metal dopant (M) and Pt, respectively.

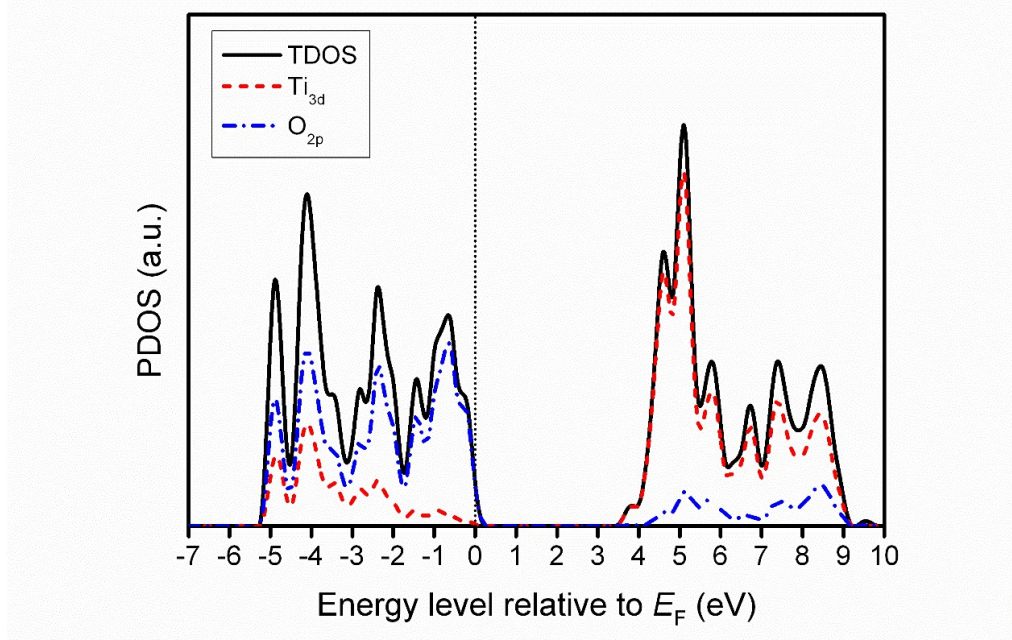
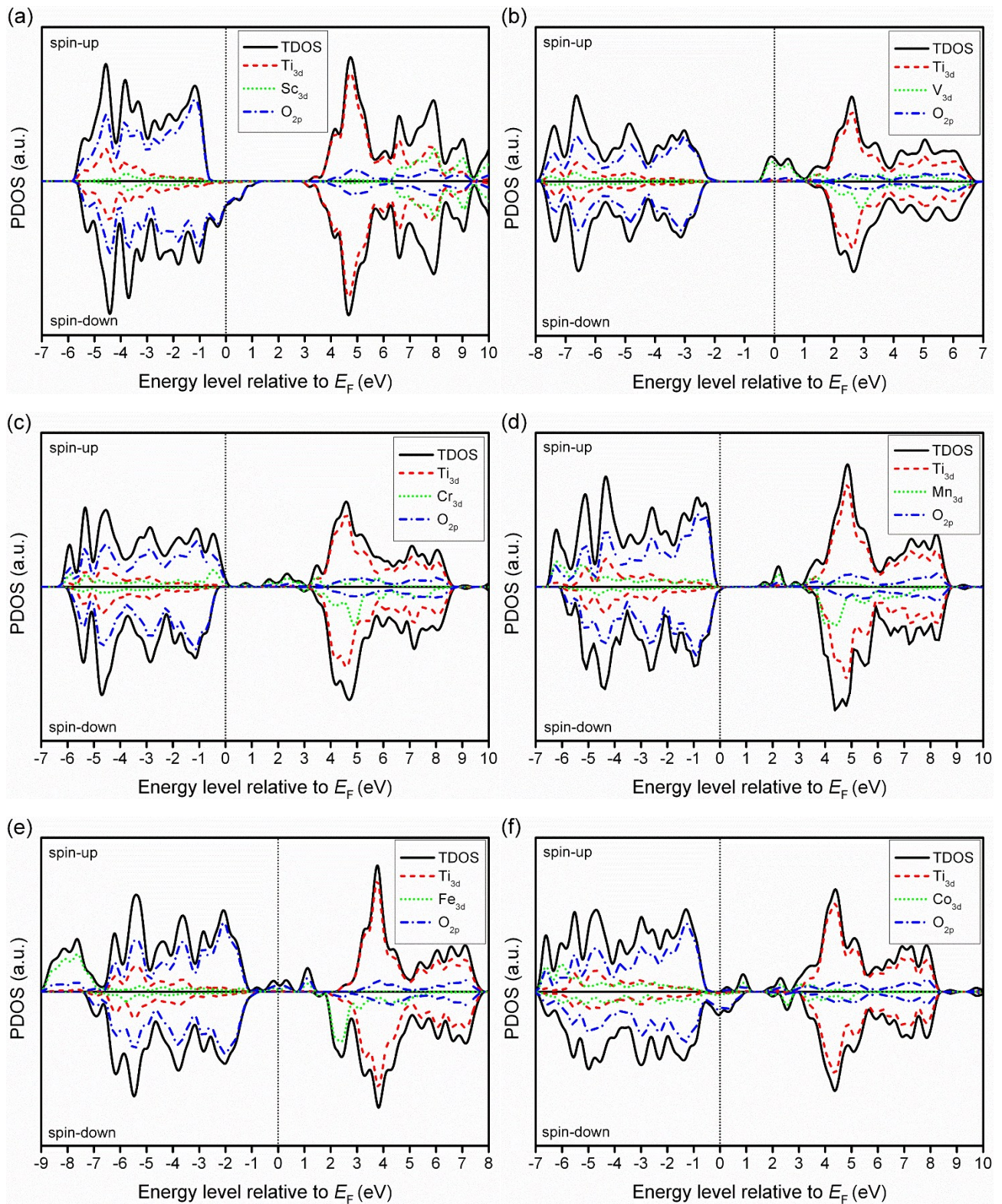


Figure S5 Calculated total and partial density of states of bulk anatase- TiO_2 . Black solid line represents total density of states, red dash and blue dash dot lines represent contributions of Ti_{3d} and O_{2p} electrons, respectively.



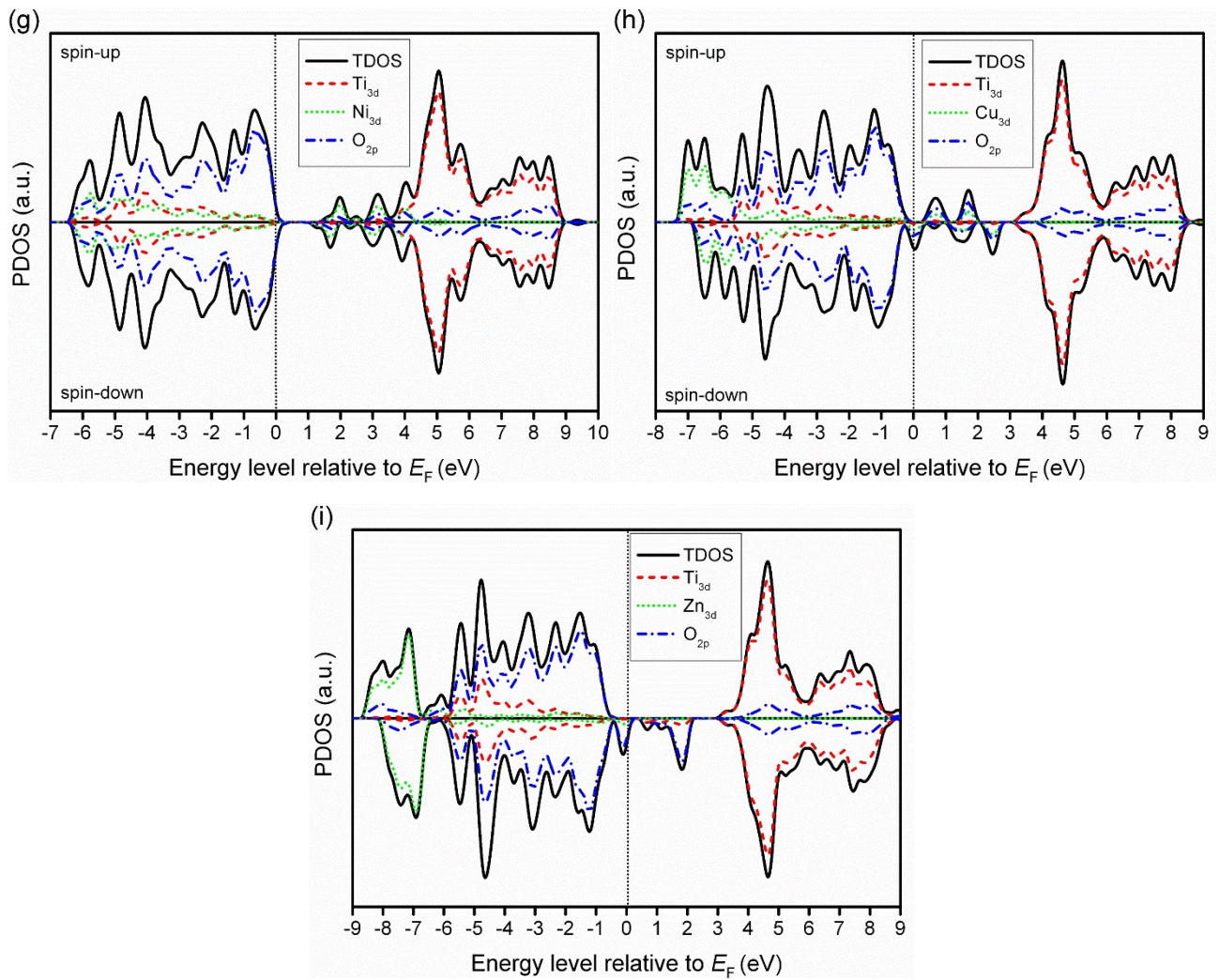
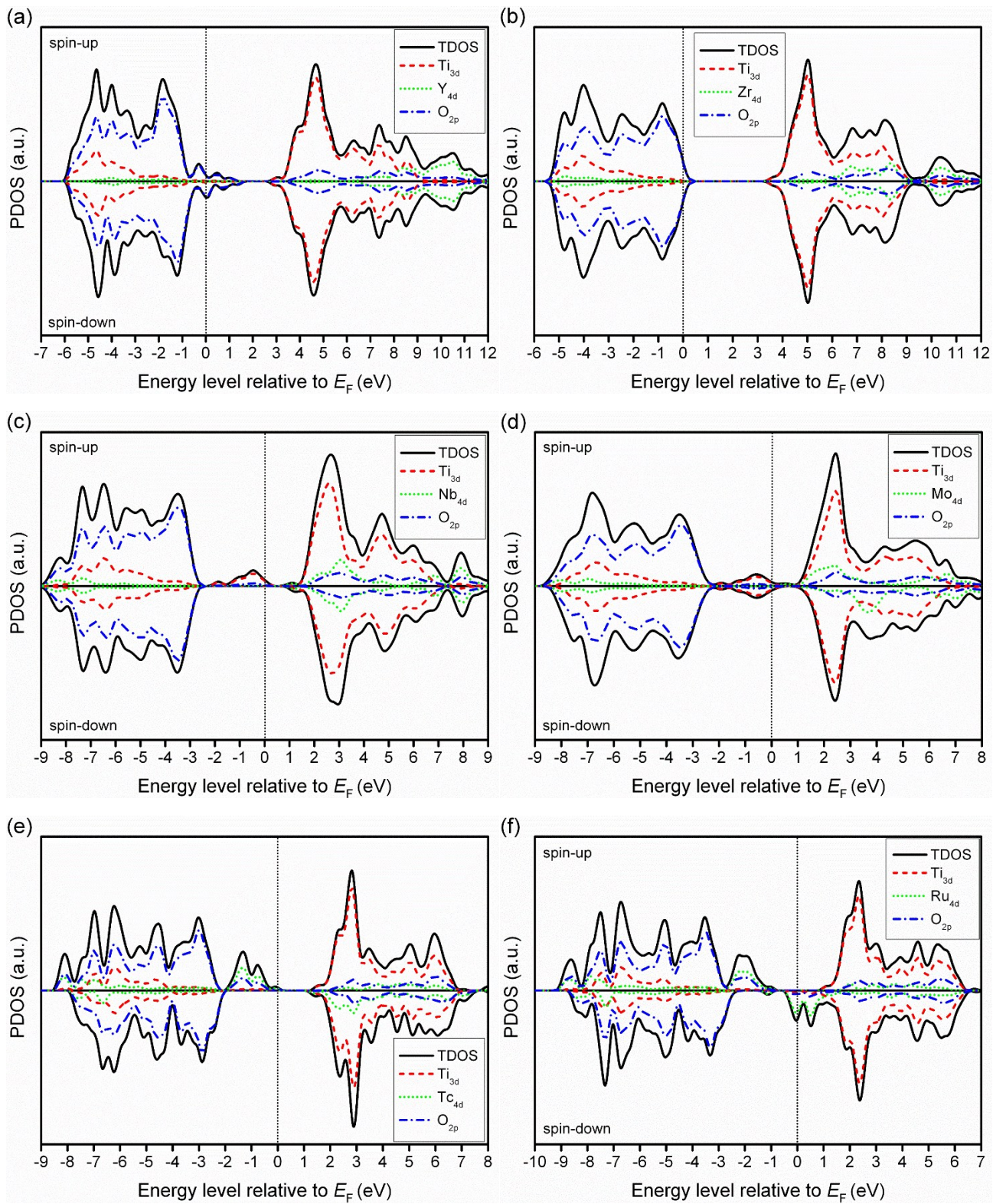


Figure S6 Calculated total and partial density of states of bulk anatase- $\text{TiM}_{3d}\text{O}_2$: (a) TiScO_2 , (b) TiVO_2 , (c) TiCrO_2 , (d) TiMnO_2 , (e) TiFeO_2 , (f) TiCoO_2 , (g) TiNiO_2 , (h) TiCuO_2 , and (i) TiZnO_2 . Black solid line represents total density of states, red dash, green dot and blue dash dot lines represent the contributions of Ti_{3d} , M_{3d} and O_{2p} electrons, respectively.



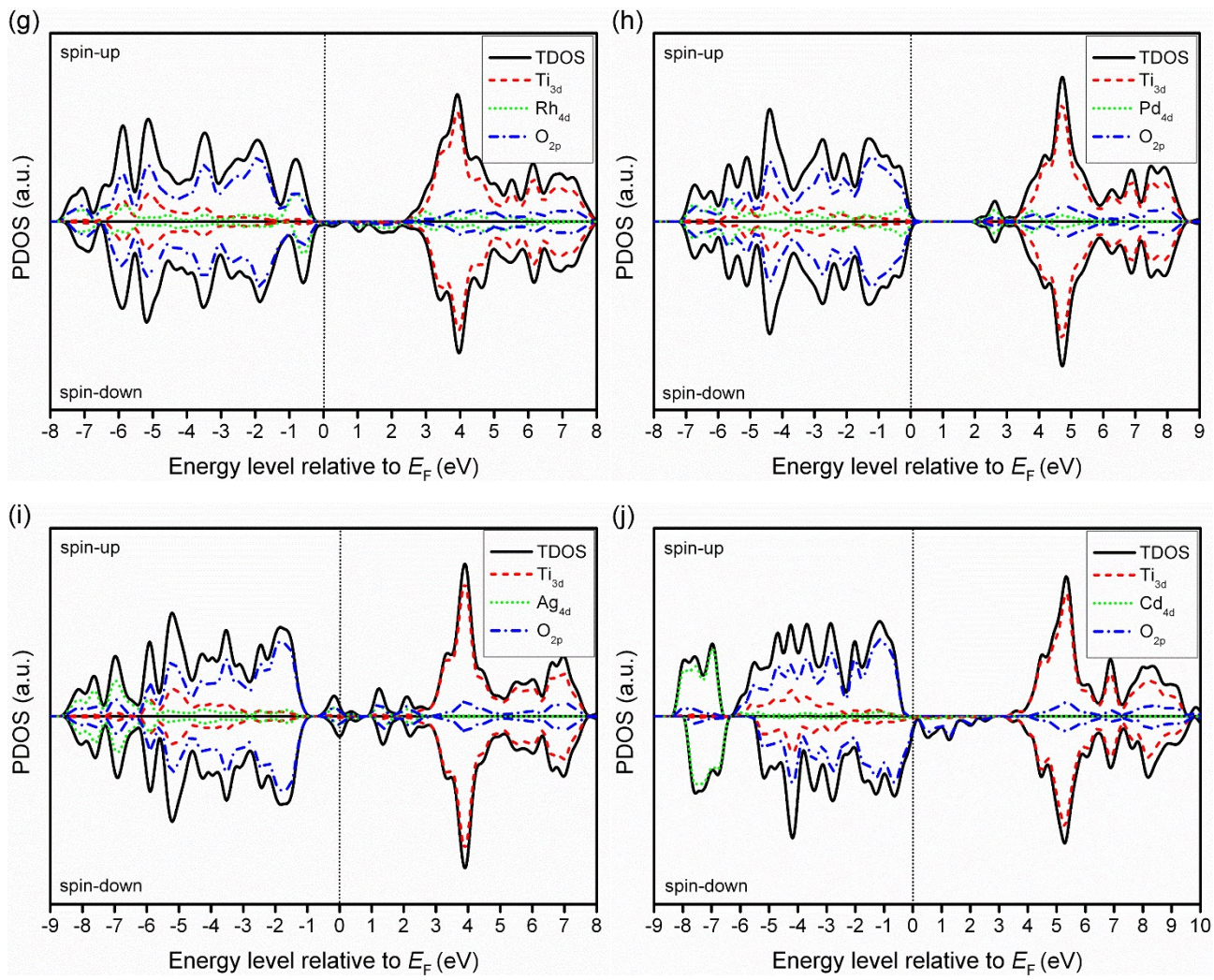
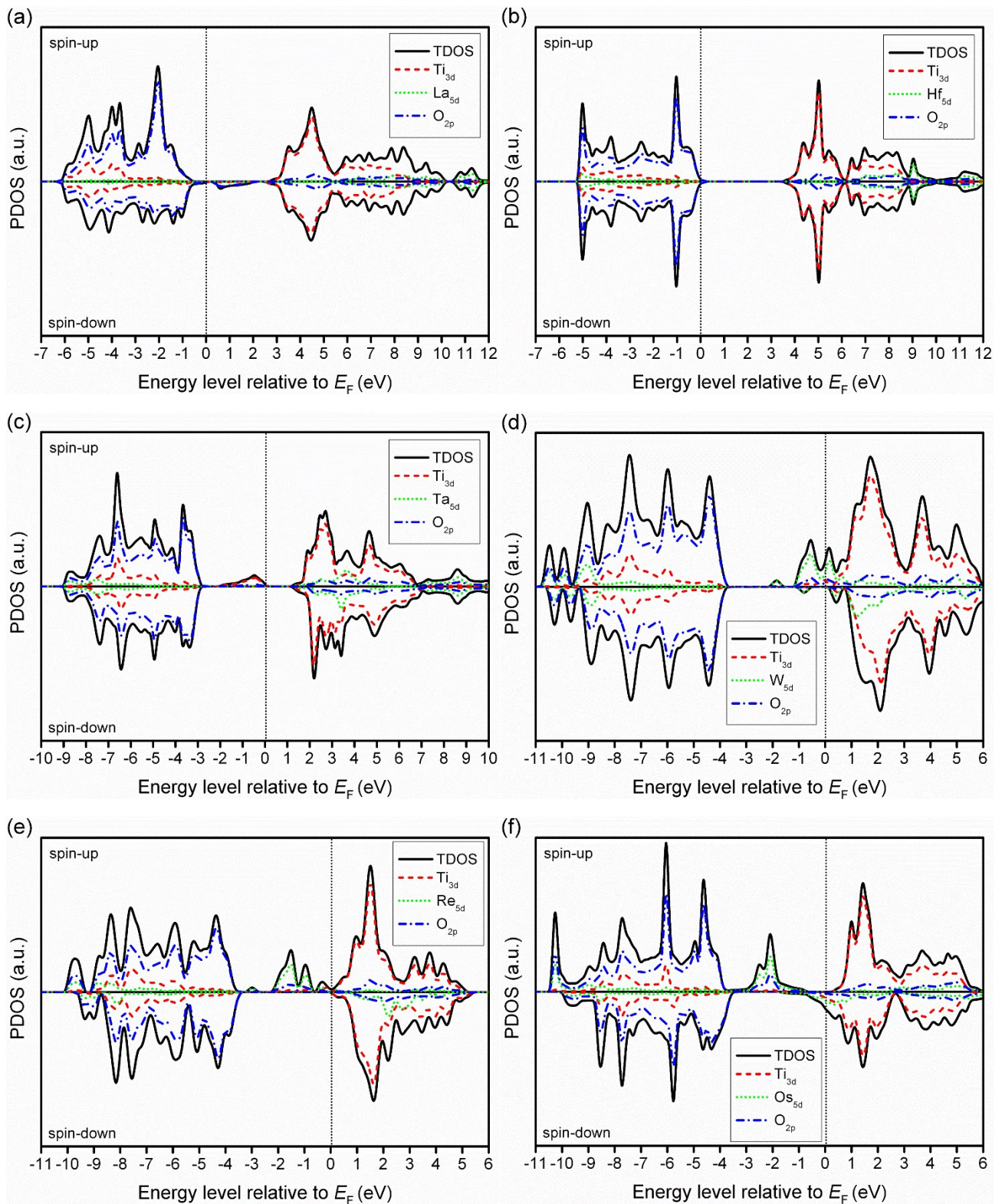


Figure S7 Calculated total and partial density of states of bulk anatase- $\text{TiM}_{4d}\text{O}_2$: (a) TiYO_2 , (b) TiZrO_2 , (c) TiNbO_2 , (d) TiMoO_2 , (e) TiTcO_2 , (f) TiRuO_2 , (g) TiRhO_2 , (h) TiPdO_2 , (i) TiAgO_2 , and (j) TiCdO_2 . Black solid line represents total density of states, red dash, green dot and blue dash dot lines represent contributions of Ti_{3d} , M_{4d} and O_{2p} electrons, respectively.



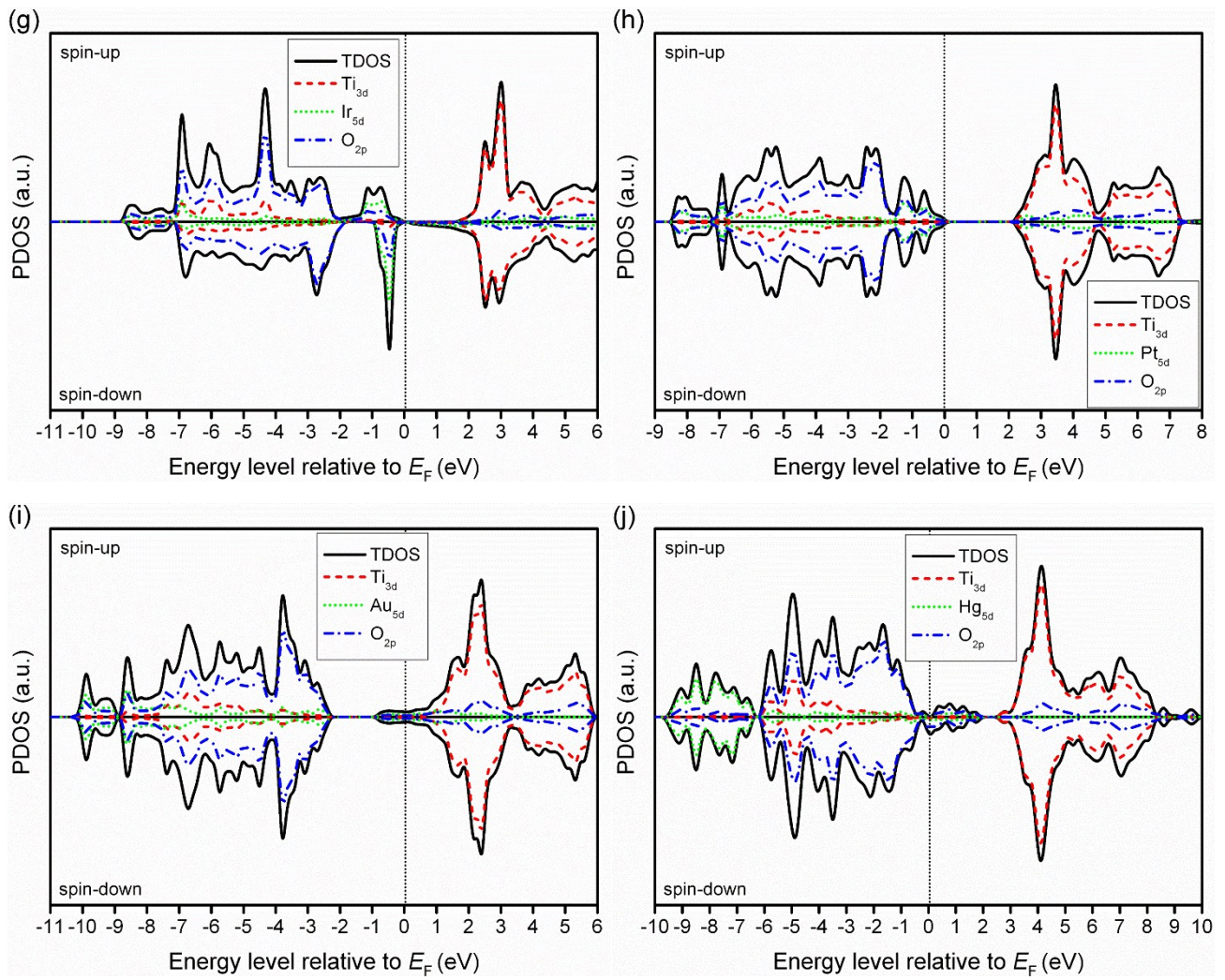


Figure S8 Calculated total and partial density of states of bulk anatase-TiM_{5d}O₂: (a) TiLaO₂, (b) TiHfO₂, (c) TiTaO₂, (d) TiWO₂, (e) TiReO₂, (f) TiOsO₂, (g) TiIrO₂, (h) TiPtO₂, (i) TiAuO₂, and (j) TiHgO₂. Black solid line represents total density of states, red dash, green dot and blue dash dot lines represent contributions of Ti_{3d}, M_{5d} and O_{2p} electrons, respectively.

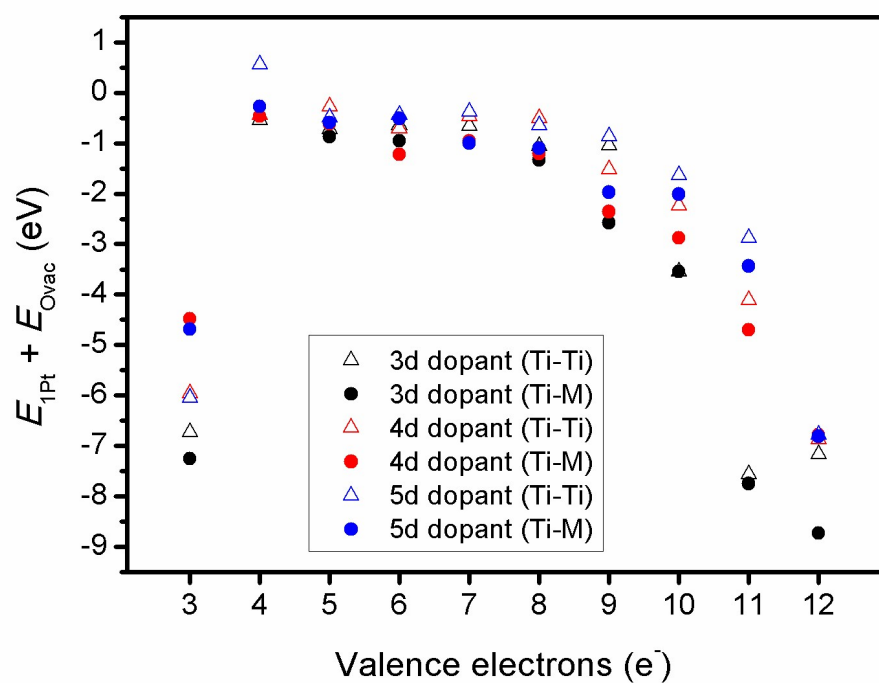


Figure S9. Energy difference of $E_{1\text{Pt}}$ and E_{Ovac} , indicates that whether the adsorption of Pt atom is thermodynamically favorable on defect site, i.e. negative value means Pt favors defect site. Y axis:

$$\Delta E_{1\text{Pt}}^* = E_{1\text{Pt}} + E_{\text{Ovac}}$$

Table S1 Bader charge analysis for Ti ions of anatase-TiMO₂ obtained by HSE method.

TiM _{3d} O ₂	$\delta_{\text{Ti}} / \text{e}^-$	TiM _{4d} O ₂	$\delta_{\text{Ti}} / \text{e}^-$	TiM _{5d} O ₂	$\delta_{\text{Ti}} / \text{e}^-$
TiScO ₂	1.1284	TiYO ₂	1.1231	TiLaO ₂	1.1171
TiO ₂	1.1491	TiZrO ₂	1.1265	TiHfO ₂	1.1159
TiVO ₂	1.1391	TiNbO ₂	1.2616	TiTaO ₂	1.2909
TiCrO ₂	1.1396	TiMoO ₂	1.1359	TiWO ₂	1.3229
TiMnO ₂	1.1377	TiTcO ₂	1.1315	TiReO ₂	1.1430
TiFeO ₂	1.1309	TiRuO ₂	1.1579	TiOsO ₂	1.1666
TiCoO ₂	1.1426	TiRhO ₂	1.1526	TiIrO ₂	1.1384
TiNiO ₂	1.1469	TiPdO ₂	1.1345	TiPtO ₂	1.1342
TiCuO ₂	1.1396	TiAgO ₂	1.1283	TiAuO ₂	1.1368
TiZnO ₂	1.1283	TiCdO ₂	1.1146	TiHgO ₂	1.1369

Table S2 Pt/TM-doped TiO₂ applied in fuel cell reactions

Catalyst system	Electrical conductivity (S/cm)	Support composition	Electron transfer	application	Year, ref
Pt/TiNbO ₂	0.1	NA	Support to Pt	ORR	2007 ¹
Pt/TiNbO ₂	6.1×10 ⁻⁴	Ti _{0.9} Nb _{0.1}	NA	ORR	2009 ²
Pt/TiNbO ₂	1.11 (900°C)	Ti _{0.75} Nb _{0.25} O ₂	NA	ORR	2010 ³
Pt/TiMoO ₂	2.8×10 ⁻⁴	Ti _{0.7} Mo _{0.3} O ₂	Support to Pt	ORR	2011 ⁴
Pt/TiMoO ₂	2.8×10 ⁻⁴	Ti _{0.7} Mo _{0.3} O ₂	Support to Pt	ORR	2016 ⁵
Pt/TiTaO ₂	0.2	Ti _{0.7} Ta _{0.3}	NA	ORR	2013 ⁶
Pt/TiTaO ₂	0.2	Ti _{0.7} Ta _{0.3}	Support to Pt	ORR	2014 ⁷
Pt/TiCrO ₂	Good but no value indicated	Ti _{0.95} Cr _{0.05}	Support to Pt	ORR	2014 ⁸
Pt/TiTaNbO ₂	8.73×10 ⁻⁴	Ta _{0.08} Nb _{0.2}	Electronic transfer is important	ORR	2014 ⁹
Pt/TiRuO ₂	NA	Ti _{0.7} Ru _{0.3} O ₂	Support to Pt	MOR	2011 ¹⁰
Pt/TiRuO ₂	Good but no value indicated	Ti _{0.9} Ru _{0.1} O ₂	NA	MOR, CO stripping	2015 ¹¹
Pt/TiWO ₂	0.02-0.9	Ti _{0.7} W _{0.3} O ₂	NA	ORR	2010 ¹²
Pt/TiWO ₂	0.02-0.9	Ti _{0.7} W _{0.3} O ₂	NA	HOR, CO stripping	2010 ¹³
Pt/TiWO ₂	Adding carbon to ensure sufficient conductivity	Ti _{0.7} W _{0.3} O ₂	Support slightly modifies Pt electronic structure	HOR, CO stripping	2015 ¹⁴

1. K.-W. Park and K.-S. Seol, *Electrochem. Commun.*, 2007, **9**, 2256-2260.
2. H. Chhina, S. Campbell and O. Kesler, *J. Electrochem. Soc.*, 2009, **156**, B1232-B1237.
3. S.-Y. Huang, P. Ganesan and B. N. Popov, *Applied Catalysis B: Environmental*, 2010, **96**, 224-231.
4. V. T. T. Ho, C.-J. Pan, J. Rick, W.-N. Su and B.-J. Hwang, *J. Am. Chem. Soc.*, 2011, **133**, 11716-11724.
5. M.-C. Tsai, T.-T. Nguyen, N. G. Akalework, C.-J. Pan, J. Rick, Y.-F. Liao, W.-N. Su and B.-J. Hwang, *ACS Catalysis*, 2016, **6**, 6551-6559.
6. A. Kumar and V. Ramani, *J. Electrochem. Soc.*, 2013, **160**, F1207-F1215.
7. A. Kumar and V. Ramani, *ACS Catalysis*, 2014, **4**, 1516-1525.
8. J.-H. Kim, S. Chang and Y.-T. Kim, *Applied Catalysis B: Environmental*, 2014, **158–159**, 112-118.

9. Y.-J. Wang, D. P. Wilkinson, V. Neburchilov, C. Song, A. Guest and J. Zhang, *Journal of Materials Chemistry A*, 2014, **2**, 12681-12685.
10. V. T. Thanh Ho, K. C. Pillai, H.-L. Chou, C.-J. Pan, J. Rick, W.-N. Su, B.-J. Hwang, J.-F. Lee, H.-S. Sheu and W.-T. Chuang, *Energy & Environmental Science*, 2011, **4**, 4194-4200.
11. M. D. Obradović, U. Č. Lačnjevac, B. M. Babić, P. Ercius, V. R. Radmilović, N. V. Krstajić and S. L. Gojković, *Applied Catalysis B: Environmental*, 2015, **170–171**, 144-152.
12. C. V. Subban, Q. Zhou, A. Hu, T. E. Moylan, F. T. Wagner and F. J. DiSalvo, *J. Am. Chem. Soc.*, 2010, **132**, 17531-17536.
13. D. Wang, C. V. Subban, H. Wang, E. Rus, F. J. DiSalvo and H. D. Abruña, *J. Am. Chem. Soc.*, 2010, **132**, 10218-10220.
14. D. Gubán, I. Borbáth, Z. Pászti, I. Sajó, E. Drotár, M. Hegedűs and A. Tompos, *Applied Catalysis B: Environmental*, 2015, **174–175**, 455-470.